Sensors & Diagnostics

PAPER

View Article Online
View Journal | View Issue

Cite this: *Sens. Diagn.*, 2024, **3**, 827

Fiber-optic probes for real-time pH monitoring†

Mohamed Elsherif, *[ab] Fahad Alam,[ac] Ahmed E. Salih,[a] Xinyu Wang,[d] Peter R. Corridon, [efg] Khalil B. Ramadi[bh] and Haider Butt*[a]

While pH determination is a commonplace laboratory practice, conventional commercial pH probes exhibit drawbacks of bulkiness, slow response times, and signal drift. These become particularly limiting in specialized fields like tissue engineering and bio-industrial processing, where unique pH probe specifications surpass the capabilities of standard laboratory equipment. Here, we present the development of compact pH fiber probes by integrating silica optical fiber with a colorimetric pH indicator. Our approach involves cross-linking the pH indicator with a biocompatible synthetic hydrogel matrix, facilitating colorimetric and precise pH measurements. Two distinct designs of optical fiber sensors were devised to cater to a broad spectrum of applications. The first design involved attaching the hydrogel sensor to the fiber tip during the photopolymerization process, while the second design was crafted by folding the hydrogel sensor onto the bare terminal of the fiber using the casting process. The fiber sensor exhibited high sensitivity (17 nm pH^{-1}) within physiological and pathophysiological pH ranges (6–8) when tested in reflection configuration. Validation of the developed fiber sensors was carried out on cancerous tissue phantoms derived from an ovine extracellular matrix. The unique specifications of these fiber sensors position them as promising candidates for applications in tissue engineering, cell growth, and continuous blood pH monitoring.

Received 9th January 2024,
Accepted 13th March 2024

DOI: 10.1039/d4sd00012a

rsc.li/sensors

Introduction

Determination of pH holds paramount importance across diverse applications, spanning tissue engineering, tumor diagnosis, wastewater management, biotechnology, the chemical industry, physiological processes in organisms, and intracellular regulatory scenarios.[1–6] While the pH glass electrode stands as the prevailing system, its inherent limitations, such as bulkiness, sizable sample volume requirements (10 ml), and the need for discontinuous calibration, render it unsuitable for various contexts.[7,8] Long-term continuous measurements face challenges stemming from calibration issues, electrode fouling, and clogging problems.[9]

In specific applications like tissue engineering, monitoring cell growth necessitates meticulous control of pH values.[10] Tissue engineering mandates sophisticated sensors and cell bioreactors capable of standardizing, controlling, and automating growth and testing conditions for optimal reproducibility.[11] Sustaining the desired growth environment in bioreactors entails precise control over various parameters, with pH being a critical factor.[12] Analytical sensors with high repeatability are indispensable for this purpose. As cells undergo growth, the natural acidification of their environment occurs. Maintaining an optimal pH level of around 7 is crucial, as deviations towards acidity or alkalinity can compromise cell viability.[13] Tissue engineering studies, often spanning weeks, demand continuous monitoring.[14] Commercial pH instruments prove inadequate for such applications, as conventional pH meters lose up to 0.1 pH units of accuracy daily in the absence of regular calibration.[15]

Highly spatial resolution pH sensors find *in vivo* applications, particularly in the context of tumor cells and their microenvironments characterized by their acidity. The pH in the vicinity of tumor cell surfaces registers as acidic (6.7–6.8), and this acidity progressively increases with distance from the cell membrane.[16] Unlike bulk pH measurements that might overlook tumor cells, smaller probes with enhanced spatial resolution prove instrumental

[a] *Department of Mechanical Engineering, Khalifa University, Abu Dhabi 127788, United Arab Emirates. E-mail: elsherifmohamed109@gmail.com, haider.butt@ku.ac.ae*
[b] *Division of Engineering, New York University Abu Dhabi, Abu Dhabi 129188, United Arab Emirates*
[c] *Department of Electrical and Computer Engineering, King Abdullah University (KAUST), 23955, Saudi Arabia*
[d] *Department of Biomedical Engineering, Khalifa University, Abu Dhabi 127788, United Arab Emirates*
[e] *Department of Immunology and Physiology, College of Medicine and Health Science, Khalifa University, Abu Dhabi 127788, United Arab Emirates*
[f] *Healthcare Engineering Innovation Center, Khalifa University, Abu Dhabi 127788, United Arab Emirates*
[g] *Center for Biotechnology, Khalifa University, Abu Dhabi 127788, United Arab Emirates*
[h] *Tandon School of Engineering, New York University, NY 11201, USA*
† Electronic supplementary information (ESI) available. See DOI: https://doi.org/10.1039/d4sd00012a

in delineating precise surgical margins during tumor resection. Beyond tumor-related applications, extracellular acidity has been linked to various pathologies, including ischemic, stroke, neurotrauma, epileptic seizures, inflammation, infections, and wound healing.[17–19]

Optical fiber probes, developed to address the limitations of glass electrodes, offer distinct advantages such as remote sensing, immunity to electromagnetic interference, minimal contact area, and significantly reduced sample size (1 μl).[20] These fiber sensors rely on changes in the optical properties (absorbance or fluorescence) of the pH-sensitive segment, responding to variations in pH.[20,21] Among optical sensors, fluorescence sensors stand out for their simplicity, high sensitivity, and specificity.[22] In this system, the fluorophore undergoes intensity changes during reversible protonation/deprotonation, resulting in an optical response governed by the Henderson–Hasselbalch equation.[23] This yields a sigmoidal response function with a dynamic working range, enabling pH determination within specific pH windows.[23–29] Fluorescence-based pH sensors find applications in diverse fields such as the environment, biological research, industry, and disease diagnosis.[30] However, direct fluorescence measurements are susceptible to background light interference and photo-bleaching.[31] In contrast, absorbance-based pH sensors, perceptible to the naked eye, are straightforward.[20] Yet, challenges arise from potential pH indicator leakage when physically trapped in the hydrogel or poor response when chemically crosslinked in the hydrogel matrix.[32–35]

Neutral red (NR), a widely employed pH indicator in biology, is commonly immobilized in sensitive hydrogels or films.[36] Its commendable performance as a water-soluble colorimetric pH indicator, functioning within the physiological pH range, has positioned NR as a preferred choice in pH sensor applications.[22,23] Previous studies have involved the immobilization of NR dye in various matrices, including agarose films, cellulose acetate, and a copolymer of allylamine hydrochloride and polyacrylic acid.[32,34,37,38] Nevertheless, it's crucial to note that the hydrogel matrix employed for dye entrapment undergoes pH-dependent changes, significantly impacting and potentially masking the response of the pH indicator.

In this study, neutral red (NR) was cross-linked with synthetic biocompatible hydrogel, polyhydroxy ethyl methacrylate. This hydrogel demonstrated superior resistance to harsh pH environments when compared to materials such as agarose, polyacrylic acid, and cellulose acetate, as documented in the existing literature.[32,34,38] An additional advantage of the chosen matrix is its non-interference with the colorimetric response of the pH indicator, a limitation observed in prior research.[32,34,38] Furthermore, the selected hydrogel matrix ensures the pH indicator's stability, preventing leakage under operational conditions within both physiological and pathological pH ranges. This study presents two distinct designs: firstly, the attachment of the hydrogel to the fiber tip, yielding a system that does not necessitate a large contact area or sample volume; secondly, the wrapping of the hydrogel on the fiber terminal, designed for prolonged sensing applications. The practicality of these fiber sensors was demonstrated through testing in reflection configuration. Validation was conducted through application on models of healthy and cancerous tissue phantoms.

Results and discussion

We selected neutral red dye to be the pH indicator in the developed sensors because of its working range (pH of 6–8) which makes it ideal for physiological and pathophysiological pH sensing applications.[36] Neutral red is a eurhodin dye used for staining in histology and is also called toluylene red, basic red 5, and C.I. 50040.[39] The chemical structure of NR responds to the medium pH changes leading to shifting the dye color from red to yellow when pH changes from acidic to basic (Fig. 1a). Prior to immobilizing the dye into the hydrogel, the dye was dissolved in aqueous solutions of different pH values (5, 6, 7, and 8) and the spectral responses of the dye solutions were recorded using a spectrometer (Fig. 1). As predicted, the dye color was red in the acidic solutions of pH 5 and 6, and it turned yellow in the basic solution of pH 8 (Fig. 1b). The absorption spectra of the NR solutions showed absorption peaks at wavelengths of 522, 520, 495, and 480 nm, for aqueous solutions of pH 5, 6, 7, and 8, respectively (Fig. 1c and d). The absorption peak for the solution of pH 7 was the widest among the rest and this might be due to that the pH 7 is very close to the color-turning pH value of the NR dye which is 6.8 (Fig. 1c). The trend of the absorption peak positions *versus* pH shows the dye's colorimetric response almost saturates at pH 6 (Fig. 1d). The transmission measurements recorded for the same NR solutions completely matched the absorbance measurements. For NR solutions of pH 5, 6, 7, and 8, broad valleys were observed to be positioned at wavelengths 522, 520, 495, and 480 nm, respectively (Fig. 1e). Additionally, the valley in the transmission spectrum for the solution of pH 7 was as wide as the peak observed in the absorbance measurement for the same solution.

The pH-responsive hydrogels were synthesized using the free-radical polymerization method. The neutral red dye as the pH indicator was immobilized in a biocompatible hydrogel matrix, *i.e.*, poly (hydroxyethyl methacrylate), during the photo-polymerization process. The dye was dissolved in DI (de-ionized) water and mixed with the monomer solution, followed by photo-polymerizing the mixture in a glass mold to produce free-standing pH-responsive hydrogels. To investigate the influence of the dye solvent on the dye performance when it is immobilized in the hydrogel matrix, three more samples were prepared by dissolving NR in DMSO, ethanol, and isopropanol, separately. The prepared four samples were denoted by h_w, h_d, h_e, and h_i, which stand for the pH-hydrogel sensors prepared using DI water, DMSO, ethanol, and isopropanol as solvents, respectively. The freshly prepared free-standing hydrogel sensors were tested for pH sensing in highly acidic (pH 2) and basic (pH 12)

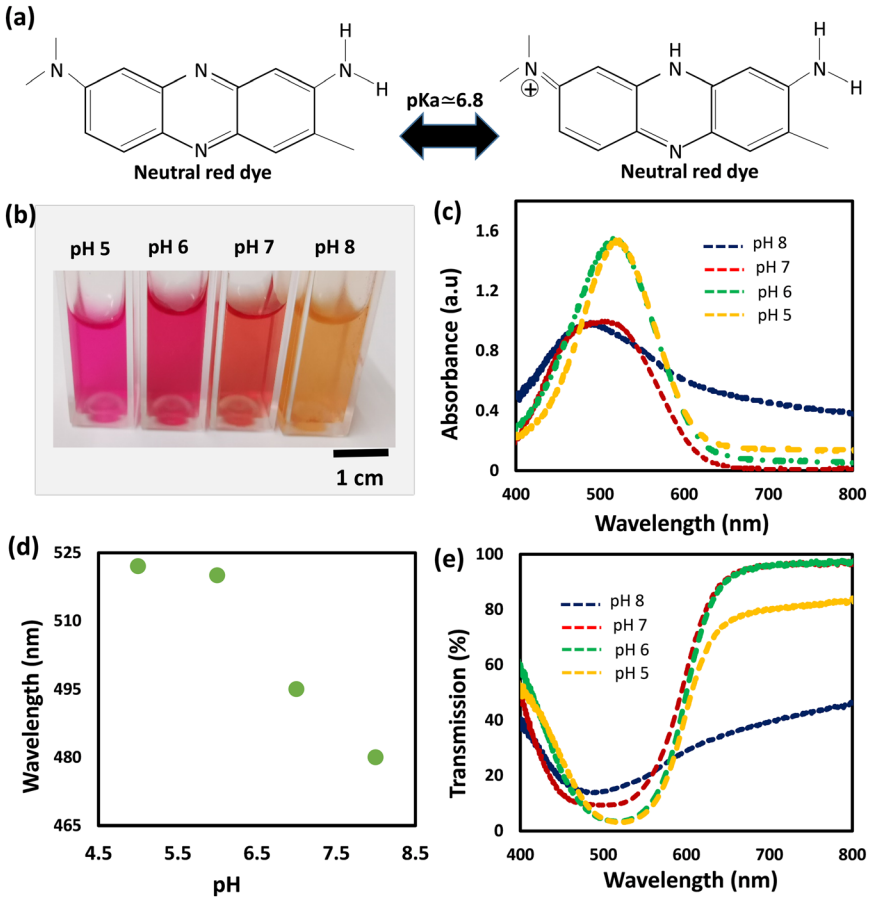

Fig. 1 Response of the neutral red dye dissolved in DI water of different pH. (a) The chemical structure of the neutral red dye in basic (left) and acidic (right) media. (b) Photograph of NR dissolved in DI water of pH values 5, 6, 7, and 8. (c) Absorption spectra of NR dissolved in DI water solutions of different pH values. (d) The absorption peak positions of the aqueous solutions of pH values 5, 6, 7, and 8. (e) Transmission spectra of NR aqueous solutions of pH values 5, 6, 7, and 8.

environments (Fig. 2). The four hydrogel sensors; h_w, h_d, h_e, and h_i, turned from red to yellow when the pH of the environment changed from 2 to 12 (Fig. 2a). These free-standing hydrogel sensors have a 500 μm thickness as confirmed by the optical microscopic images taken for their cross-section (Fig. S1†). The colorimetric responses of the hydrogel sensors were detected by measuring the light absorbance. At low pH conditions (2 units), both h_i and h_e sensors showed absorption peaks centered at the wavelength of 534 nm, while h_w and h_d sensors presented absorption peaks centered at wavelengths 525 and 530 nm, respectively (Fig. 2b). Again, at high pH (12 units), both h_i and h_e sensors presented absorption peaks centered at the same wavelength of 460 nm while the h_w and h_d sensors showed absorption peaks positioned at 447 and 456 nm, respectively (Fig. 2c). The optical response measurements confirmed that h_e and h_i sensors functioned the same, showing a peak shift of 74 nm upon changing the pH from 2 to 12 (Fig. 2d and e). Among the four prepared sensors, the h_w sensor provided the best performance, showing an absorption peak shift of 79 nm with pH changing from 2 to 12. Compared to h_i and h_e sensors, the positions of the absorption peaks for the h_d sensor were centered at different positions when tested in pH solutions of values 2 and 12; however, the shift of the peak positions with the pH changes was 74 nm, which is still the same. Based on these results, the dye solvent slightly influences the sensitivity and the response of the developed pH sensors. Previously, studies showed very high/low pH media may cause irreversible damage to the pH-sensitive hydrogel.[37] However, these developed sensors provided a highly stable optical response reflecting their high stability in harsh environments, which is an essential property for biomedical and environmental sensing applications.

Photographs of the hydrogel sensors were taken over time to show their dynamic colorimetric change from red to yellow when the sensors were immersed in a high pH solution (12 units). The photographs were captured every two minutes until the sensors' color completely changed and stabilized. First, the color change in response to pH occurred at the edges, and this change gradually expanded to cover the whole sensor's surface. The sensors responded to the pH change within 2 min and were saturated in approximately 10 min (Fig. 3). These results showed the significance of minimizing the sensor's size and thickness, which are crucial

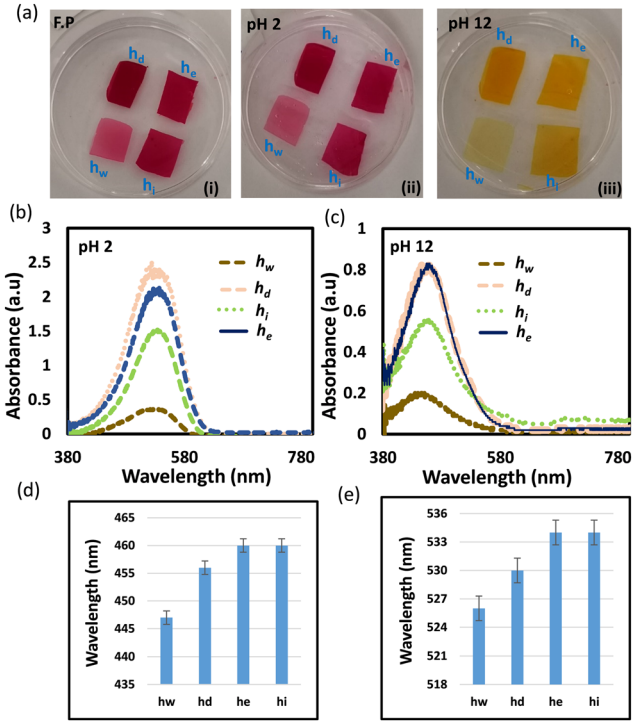

Fig. 2 Response of the pH-hydrogel sensors to low and high pH values. (a) Photographs of the four pH-sensitive hydrogel sensors; h_d, h_e, h_w, and h_i, as freshly prepared (F.P) (i), dipped in a low pH solution (2 units) (ii), and dipped in a high pH solution (12 units) (iii). (b) The absorption spectra of the four pH sensors in a low pH solution (2 units). (c) The absorption spectra of the four pH sensors in a high pH solution (12 units). (d) Positions of the absorption peaks for the four sensors immersed in a low pH solution (2 units). (e) Positions of the absorption peaks for the four sensors dipped in a high pH solution (12 units).

considerations for shortening the response and saturation times. Therefore, thinner (100 μm) sensors were prepared and shown to change their colors uniformly (Fig. S2, and ESI† videos). The optical response of the sensors at low and high pH values was recorded over time using the spectrometer (Fig. 4). Decreasing the sensors' thicknesses led to enhancement in both response and saturation times (ESI† video). The response time declined to 5 s and the saturation time became 30 s as compared to 2 min and 10 min for their counterpart thick sensors, respectively (Fig. 4a–d).

Thin hydrogel sensors (100 μm) were tested in the pH range of 5–8, and their optical responses were recorded (Fig. 5). Transmission spectra measurements for the four sensors showed significant increases in the transmittance levels in the spectral range centered around 550 nm, upon increasing the pH from 5 to 7 (Fig. 5i(a–d)). Significant shifts for the valleys' positions in the transmission spectra toward shorter wavelengths, were observed when pH changed from 7 to 8. These results are explained and supported by the absorption spectra measurements that showed a decrease in the absorbance of the hydrogel sensors with increasing pH, in addition to the blue shift of the absorption peak positions occurring at pH 8 (Fig. 5ii(a–d)). Also, the measured light intensity showed an increase in the light intensity in the spectra range around 550 nm, upon increasing pH (Fig. S3(a–d)†). Positions of the absorption peaks *versus* pH changes for the four sensors are displayed in Fig. S4.†

The h_w sensor performed the best in terms of sensitivity and showed excellent robustness that was observed during the handling of the sensor. Therefore, the h_w sensor was

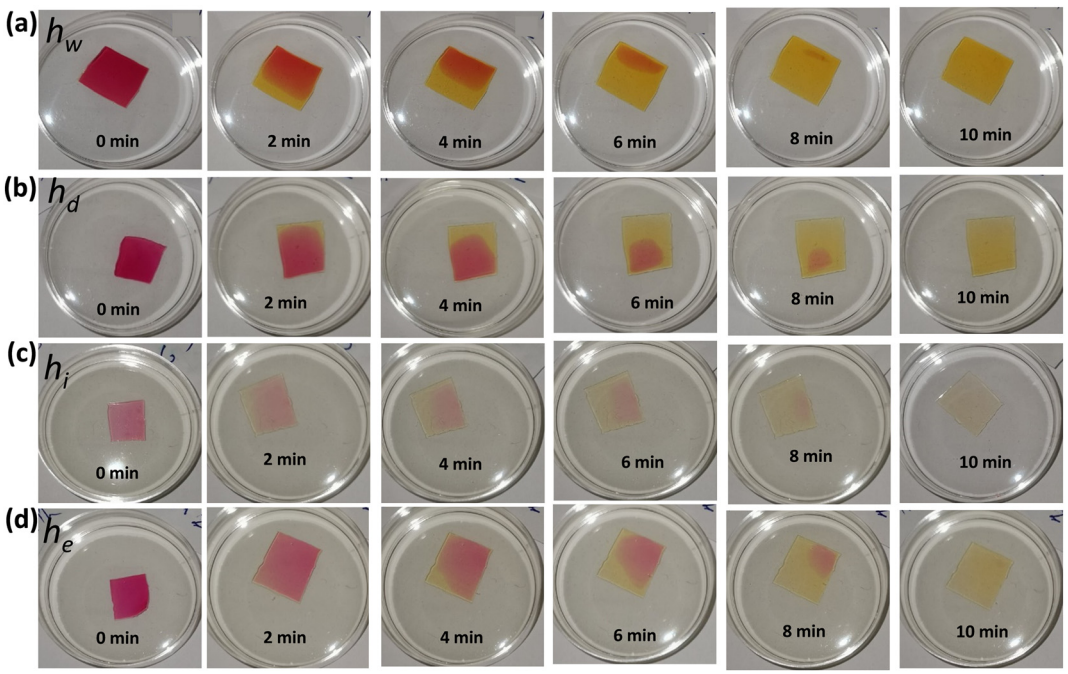

Fig. 3 Photographs were taken over time for the four thick free-standing hydrogel pH sensors while they were immersed in a solution of pH 12: (a) h_w, (b) h_d, (c) h_i, and (d) h_e.

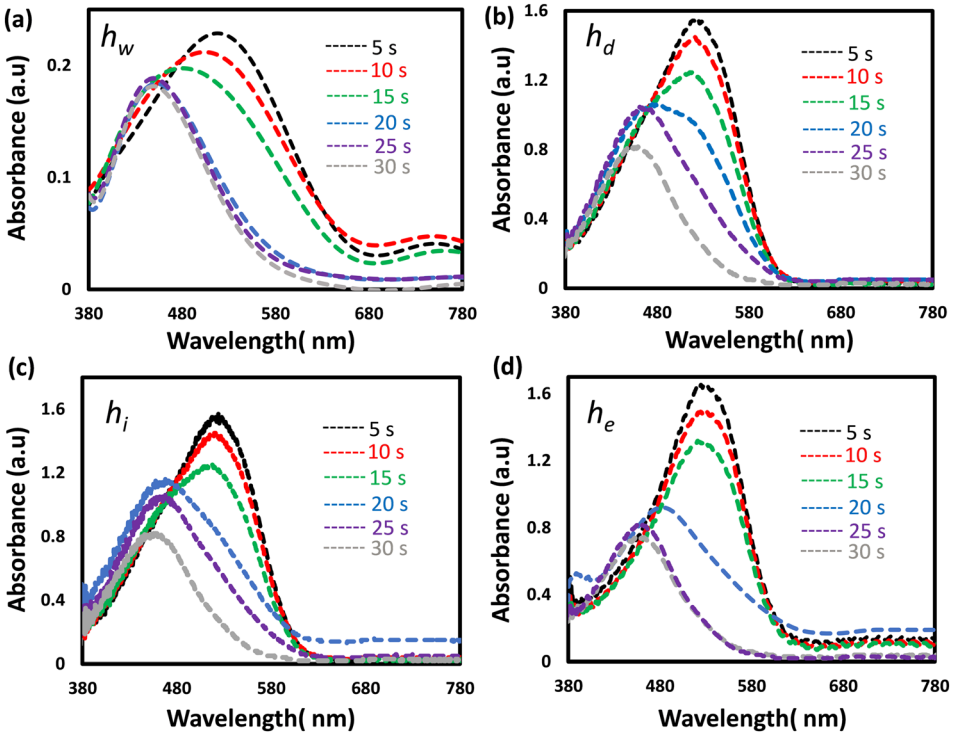

Fig. 4 The optical response recorded over time for the thin pH sensors when they were immersed in a solution of pH 12: (a) h_w, (b) h_d, (c) h_i, and (d) h_e.

taken to the next stage. Also, the stability of the sensor and its dye leachability were tested. For *in vivo* applications, the pH indicator dye must not leach out to avoid adverse inflammatory reactions. Therefore, the leachability of the NR dye from the h_w sensor was tested by storing the sensors in PBS buffer (pH 7.4), and its absorbance was examined for 12 h (Fig. S5†). The intensity of the absorbed light by the sensor was constant over the tested period reflecting zero dye leakage and stable performance. However, further studies are in progress to determine the sensor's shelf life/maximal period of stability.

For remote sensing and real-world applications, the hydrogel h_w sensor was integrated with commercial silica optical fibers for developing pH probes. Two probes were developed using the h_w sensor. The first design could handle a small sample volume (2 μl) *via* minor contact points (Fig. 6a). Such a probe would be favorable for applications such as detecting the pH environment of cells or tissues to distinguish between healthy and cancerous states. The probe was developed by chemically attaching the pH hydrogel sensor to the fiber tip (Fig. 6b). To investigate the performance of the probe, the functionalized fiber tip was dipped in different pH solutions and the other end of the fiber was connected to a three terminal-bundle fiber (Fig. 6c). A white light source illuminated the fiber, and the absorbed light was recorded by a spectrometer, in reflection configuration. The fiber sensor was stored in a buffer of pH 4 to keep it hydrated all the time, so it could be ready immediately for the measurements when needed. The absorption spectra of the fiber sensor while it was immersed in the storage buffer, were recorded as the reference spectrum, and then the fiber sensor was immersed in the tested pH solutions one by one starting from the lowest pH (5 units) and ending with the highest pH solution (8 units) (Fig. 6d). All the tested pH solutions had physiological ionic strength (150 mM) and the tests were carried out at room temperature. The absorption spectra of the fiber sensor in the tested pH buffers showed valleys that were found to shift toward the shorter wavelengths with increasing pH, similar to the case when the sensor was under free-standing conditions (Fig. 6d and 5a). This shift is due to the response of the immobilized dye to the pH changes where the dye turned from red to yellow when pH changed from 5 to 8. The depth of the valleys for the absorbed wavelengths increased with increasing pH which reflects decreasing in alkaline media. Positions of the valleys for the buffers of pH values 5, 6, 7, and 8 were located at wavelengths of 575, 565, 540, and 524 nm, respectively (Fig. 6e). The absorbance measurements were supported with the total light intensity measurements which were recorded in reflection configuration (Fig. 6f). The light intensity decreased with pH at the short wavelength range <575 nm and increased at longer wavelengths >575 nm, which is due to tuning the absorption band of the pH sensor. The shift in the absorption peak/valley for the fiber sensor with pH variations from 5 to 8 measured 51 nm, indicating a notable sensitivity of 17 nm pH^{-1}. This level of sensitivity stands out when compared to previously reported fiber pH sensors relying on colorimetric pH indicators

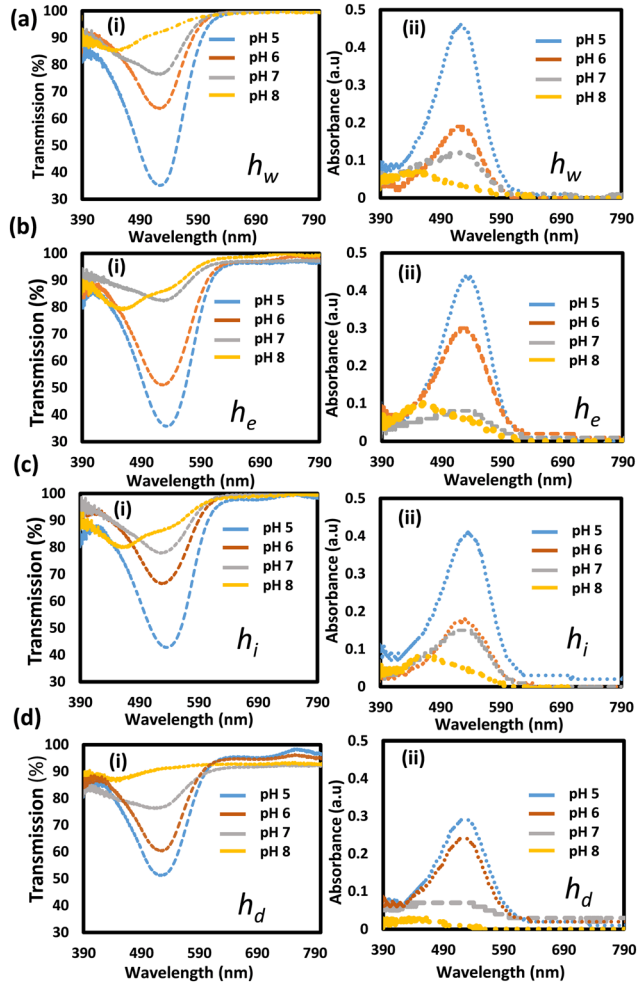

Fig. 5 Optical response of the pH-responsive hydrogel sensors. (a) The optical response of the h_w sensor while it was exposed to different pH values; (i) transmission spectra, and (ii) absorption spectra. (b) The optical response of the h_e sensor while it was exposed to different pH values; (i) transmission spectra, and (ii) absorption spectra. (c) The optical response of the h_i sensor while it was exposed to different pH values; (i) transmission spectra, and (ii) absorption spectra. (d) The optical response of the h_d sensor while it was exposed to different pH values; (i) transmission spectra, and (ii) absorption spectra.

embedded in hydrogels.[33,40,41] For instance, a fiber-optic system using the brilliant yellow dye within polyallylamine hydrochloride demonstrated a sensitivity of 5.4 nm pH^{-1}.[33] Optical fibers employing a combination of pH indicators; bromophenol blue, cresol red, and chlorophenol red, exhibited sensitivities of 1.02 and 0.93 nm pH^{-1} for acidic and alkaline media, respectively.[40] Hetero-core structure fibers utilizing phenol red and cresol red showcased a wavelength shift of 30 nm across the pH range from 2.5 to 12.7, providing a sensitivity of 3 nm pH^{-1}.[41] On the other hand, fiber pH sensors developed with the NR dye immobilized in hydrogels, such as poly(allylamine hydrochloride) and poly(acrylic acid), proved ineffective in delivering colorimetric responses to pH changes.[37,38,42,43] This ineffectiveness was attributed to the hydrogel matrices used, which masked the NR's response.

Additional experiments were carried out to study the reusability of the fiber sensor (Fig. 6g). The fiber probe was alternatively immersed in pH buffer solutions of 6 and 8 for four cycles. Highly consistent behavior and negligible drift were detected with rapid fiber response times of approximately 5 s (Fig. 6g). The kinetic response of the probe was recorded for a complete cycle in pH 6 and 8 buffers which confirms the probe's short response time (5 s) (Fig. S6†).

The second design of the fiber pH sensor was also developed and tested for pH measurements in the pH range of 5–8. A schematic illustration and photographs of the fiber sensor design are shown in Fig. 7a. In this design, the pH-responsive hydrogel wrapped the stripped terminal of the fiber (1.5 cm), and a silver paste coated the fiber tip to reflect the light increasing the sensor's light exposure for enhancing the absorbance and subsequently, the sensitivity. To investigate the fiber sensor's performance, it was immersed in a buffer of pH 4 and the measured absorbance was recorded as a reference. The light absorbance by the sensor was high when the sensor was exposed to low pH environments, and is the same as it was observed during testing of the free-stand sensors (Fig. 5a). The sensor's absorbance was the highest when it was dipped in the reference buffer of pH 4 and decreased with increasing pH. Therefore, taking the buffer of pH 4 as a reference made the absorption spectra for the pH buffers of higher pH to appear in the negative section of the *Y*-axis as the absorbance of the fiber sensor goes down with pH (Fig. 7b). The deeper the valley, the less light is absorbed by the fiber sensor as compared to the absorbance in the reference buffer, which appeared for the buffer of pH 8. Two valleys appeared in the absorbance measurements; the first was fixed at wavelength 445 nm with only light intensity change with pH, and the second valley was shifted and its intensity changed with pH. The first valley/dip may be due to the background light and the second valley was the considerable one for sensing. The light absorbance of the valleys was recorded to be −0.83, −0.96, −1.19, and −1.26 au for buffers of pH values 5, 6, 7, and 8, respectively, and the position of dips shifted from 582 to 573 nm (Fig. 7c and d). The fiber sensor showed a sensitivity of 3 nm pH^{-1} which is quite low compared to that for the first design. This difference may be due to fewer light modes propagating through the cladding made of the pH-responsive hydrogel. This issue may be overcome by tapering the terminal of the fiber before folding it with the sensor. Stretching the fiber under heat could taper the fiber terminal to achieve the best performance. The usage of a hetero-core fiber by splicing the multimode fiber terminal with a single-mode fiber coated with the pH-responsive hydrogel may have a positive influence on the probe performance too.

The second probe design offers a large fiber-to-sensor surface contact area, which assists in keeping the sensor attached to the fiber for a long period as compared to the first design. Also, the developed fiber sensor is impervious to stray light and light source fluctuations.

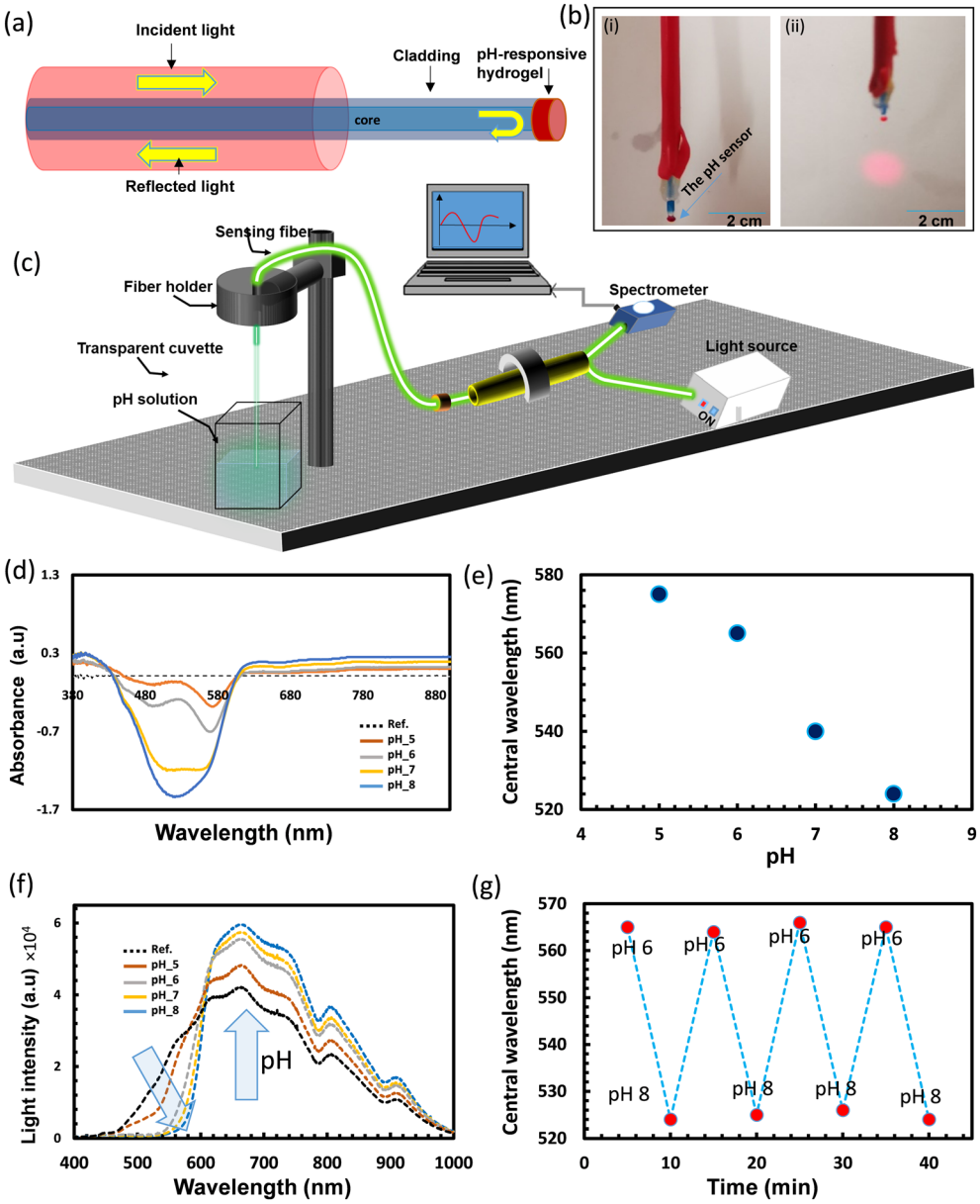

Fig. 6 Testing the optical fiber sensor of the functionalized tip. (a) Schematic illustration of the optical fiber sensor. (b) Photographs of the optical fiber sensor in OFF (i), and ON condition (ii). (c) Schematic illustration of the setup used to test the performance of the fiber sensor. (d) The absorption spectra recorded when the fiber sensor was immersed in different pH buffers. (e) The central wavelength of the valleys when the fiber sensor was dipped in different pH buffers. (f) The total light intensity reflected in the fiber while the fiber sensor was examined in different pH buffers. (g) Response of the fiber sensor when it was tested for four cycles in pH 6 and 8.

Cancer and healthy tissue models were used to demonstrate the feasibility of using the developed fiber probe for tissue differentiation applications (Fig. 8). The fiber probe of the functionalized tip was left to stabilize in a buffer of pH 7, and the reading of the fiber sensor was recorded as the reference spectrum. Then, the fiber sensor was brought in contact with the cancer model tissue, and the absorption spectrum was recorded in reflection configuration (Fig. 8a(i and ii)). Next, the probe was brought to touch the healthy (control) tissues and its response was recorded and compared (Fig. 8b). The light absorption recorded for the sensor when it was in contact with the cancerous tissues, was in the positive section of the *y*-axis, reflecting the increase in the absorbance of the sensor as compared to the sensor's absorbance while it was immersed in the reference buffer (pH 7). On the other side, the absorbance decreased as compared to the reference buffer when the sensor was in contact with the healthy tissues, shifting the absorption spectrum to the negative section of the *y*-axis and showing a valley at a wavelength of 500 nm. These results match the response of the sensor in the previous experiments as it was observed that the light absorbance decreased with pH. Consequently, for the cancerous tissues that have an acidic pH (3 units), the sensor's absorbance is more than in the

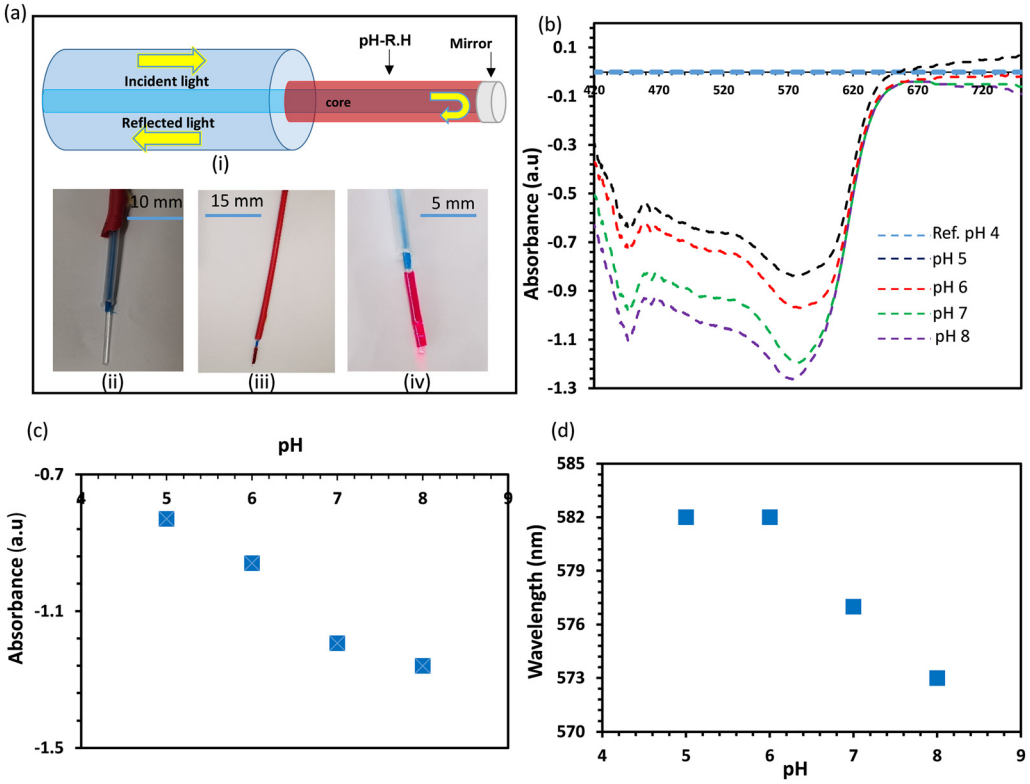

Fig. 7 Testing the pH fiber sensor of the functionalized terminal. (a) Schematic diagram demonstrating the fiber sensor (i), a photograph of the fiber before the functionalization (ii), a photograph of the functionalized terminal (iii), and a photograph of the fiber sensor illuminated with a white light (iv). (b) The fiber sensor response in different pH buffers; the test was carried out in reflection mode. (c) Light absorbance of the tested fiber sensor *versus* the pH buffers. (d) The central wavelength of the absorption band of the fiber sensor *versus* pH.

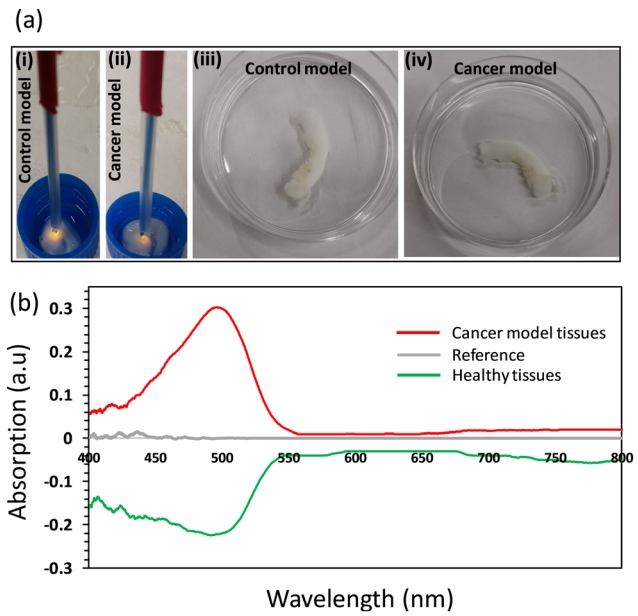

Fig. 8 Testing the fiber probe on healthy and cancer model tissues: (a) photographs of the fiber probe while it was in contact with healthy (i) and cancer model tissues (ii), and photographs of the healthy and cancer model tissues in Petri dishes (iii and iv). (b) The optical response of the fiber probe was recorded in reflection configuration while the probe was in contact with the healthy and cancer model tissues.

case of the healthy tissues that have normally alkaline pH (7.4). Based on these proof-of-concept results, the developed sensor may have the potential to discriminate between cancerous and normal tissues; however, further studies need to be performed.

Compared to the previous fiber sensors based on NR, the developed fiber sensor provided a colorimetric response with pH changes and stability in harsh pH environments.[37,38,42,43] According to the literature, the hosting materials/hydrogels for the NR dye were not passive and masked the colorimetric response of the NR dye for pH changes, hence only the absorbed light intensity changed with pH.[37,42,43] For the reported fiber, its colorimetric response to pH changes ensures that the fiber sensor is immune to instabilities, such as light source drift. Unlike the electrochemical pH sensor, the developed sensor is insensitive to electrical interference and does not require a separate reference sensor.[44] The minute dimensions of the fiber pH sensors make them appropriate to be directly placed in arteries, veins, or tissues for real-time and continuous monitoring.[45] The developed pH sensor can be integrated with the present in-dwelling medical devices, such as catheters, which would lower the barriers to adoption through subtle modifications to the existing clinician behavior. The real-time monitoring of pH is beneficial in many situations.[46] For example, blood and tissue pH would change rapidly during thoracoscopic surgery

for some patients, which could be missed by relying on intermittent laboratory measurements.[46,47] Also, the current techniques for blood pH measurements rely on *in vitro* analysis methods performed intermittently on hand-drawn samples providing only a snapshot of blood pH fluctuations.[47] However, blood pH levels may vary within minutes, and failing to monitor the short-term dramatic alterations can lead to significant patient deterioration.[47]

Conclusion

Optical fiber pH sensors were successfully developed based on a colorimetric pH indicator and a passive biocompatible hydrogel matrix. Two designs of the fiber pH sensors were developed; one model was produced by chemically attaching the sensor to the fiber tip, and the other design was made by folding the pH sensor on the bare terminal of the optical fiber. The first one is ideal for minute sample volumes and the second design fits for long-term monitoring applications. The fiber pH sensors showed a high sensitivity (17 nm pH^{-1}) and a good linear response to pH changes within the physiologically relevant pH range between 6–8. A rapid response of 5 seconds and a saturation time of 30 seconds were recorded for the thin sensors. The fiber probe was validated by application in cancer model tissues. Biofouling may limit probe functionality in *ex vivo* or *in vivo* applications such as blood pH monitoring. This challenge can be mitigated by incorporating anticoagulant agents into the hydrogel matrix or by enclosing the sensor within a membrane. However, the impact on probe performance requires thorough investigation. Hemoglobin fluorescence (580–650 nm) may also introduce interference, necessitating additional calibration steps. In extracellular pH monitoring for tumor cell diagnosis, direct tissue contact may hinder signal observation.

Materials and methods

Materials

Ethylene glycol dimethacrylate (EGDMA) 98%, 2-hydroxyethyl methacrylate (HEMA) 97%, 2-hydroxy-2-methylpropiophenone (HMPP) 97%, dimethyl sulfoxide (DMSO), sodium phosphate monobasic (99%), and sodium phosphate dibasic (99%) were purchased from Sigma Aldrich and used without any further purification.

Tissue models

Tissue models were employed in this study, and no live vertebrates were utilized. The Animal Research Oversight Committee (AROC) at Khalifa University of Science and Technology approved the experiments involving animal tissues under protocol # A20-001.

Intact aortic segments spanning the ascending to the descending portions of an Arabian sheep (Najdi, Awassi (Nuaimi), and Orb breed), were provided by a butchery (Fig. S4a†). Aortas with diameters of approximately 1.5 cm were sectioned into 2–3 cm segments and immersed in a 4% zwitterionic biosurfactant solution (Ecover, Malle, Belgium) that consisted of 15–30% non-ionic surfactants, 5–15% anionic surfactants, ethanol, sodium citrate, glycerin, trisodium ethylenediamine dissociate, polypropylene terephthalate, and citric acid. After 4 days, the tissue sections were removed from the decellularizing biosurfactant and immersed in a water bath (pH approximately 7.5) for 3 days to remove traces of the detergent. The decellularized aortic segments composed of the extracellular matrix, were placed in a freshwater bath. The aortic sections were separated into normal (the decellularized tissue scaffold) and cancerous groups. The cancerous group contained tissue segments immersed in hydrochloric acid solutions with a pH of 2.82 for 7 days to generate scaffolds with a pH of 2.99.

Preparation of the free-standing pH hydrogel sensor

HEMA monomer was mixed with PEGDA with a ratio of 10 : 1 and HMPP was added to the mixture with a ratio of 1 : 100. Neutral red was dissolved separately in DI water, DMSO, isopropanol, and ethanol. The dye solution was mixed with the monomer solution at a ratio of 1 : 4 to form the pH-responsive gel. The gel was poured into a glass mold of a spacer for the photo-polymerization to produce four pH sensors denoted as h_w, h_d, h_i, and h_e, based on the solvent used for dissolving the neutral red dye, *i.e.*, DI water, DMSO, isopropanol, and ethanol. The photo-polymerization was carried out in a UV oven (wavelength: 360 nm) for five minutes. The prepared hydrogel films were left in DI water for 2 h to be easily detached from the mold. Then, the hydrogel films were washed thoroughly three times with 50% ethanol/DI water to remove the un-polymerized materials.

Preparation of the pH testing buffers

For the testing buffers of pH in the range of 5–8, sodium phosphate monobasic solution was mixed with sodium phosphate dibasic solution. Both solutions were prepared to have a physiological ionic strength of 150 mM. The stock sodium phosphate monobasic solution had a pH of 4.2 and the sodium phosphate dibasic solution had a pH of 8.8. The appropriate volumes of each solution were mixed to prepare the pH testing buffers. For the high alkaline (pH 12) solution and the high acidic solution (pH 2), sodium hydroxide and acetic acid were used, respectively.

Fabrication of the optical fiber sensor with the functionalized tip

A droplet of 2 μl size was pipetted on a hydrophobic substrate and the silanized fiber tip was brought very close to the substrate to contact the droplet. Then, the gel was exposed to UV light for 5 min. Next, DI water was pipetted on the functionalized tip and left for 2 h to easily detach the fiber tip from the substrate. Finally, the fiber tip was washed thrice in ethanol/water at 50% vol to remove the unpolymerized materials.

Fabrication of the optical fiber sensor with the functionalized terminal

The protective coating for the silica fiber and the cladding were removed. The stripped terminal of the fiber of length 1.5 cm was thoroughly cleaned with acetone. Then, the terminal was silanized to allow chemical attachment of the hydrogel on the fiber surface. A silicon tube was used as a mold to fold the bare fiber terminal with the hydrogel matrix. The pH-responsive gel filled the tube, and the stripped terminal was inserted and cured by UV light for 5 min. Next, the tube was cut longitudinally with a blade to take out the fiber terminal. Finally, the fiber terminal was washed to be ready for the interrogation. Another way to functionalize the fiber's terminal: a platinum-cured silicone tube was used to wrap the bare fiber's core with the pH-responsive hydrogel. The bare fiber's terminal was inserted in the tube filled with the pH monomer solution and the UV curing process was initiated. After that, the tube was exposed to dichloromethane to facilitate detaching the fiber's terminal from the tube.

Testing the free-standing pH hydrogel sensors

Photographs of the prepared hydrogels were taken by a smartphone camera while the hydrogel sensors were immersed in different pH solutions and light absorption and transmission were recorded using a UV-vis spectrometer (USB 2000+, Ocean Optics) attached to an optical microscope.

Testing the optical fiber sensor

An optical setup that combines a white light source (Halogen HL-2000, ocean optics), spectrometer, and 3-terminal bundle fiber, was constructed and the optical fiber sensor was attached to the terminal of the bundle to be interrogated in reflection configuration. The other two arms of the 3-terminal bundle were connected to the spectrometer and the light source.

Author contributions

Mohamed Elsherif: conceptualization, writing-original draft, investigation, methodology, data curation, and formal analysis. Fahad Alam and Ahmed E. Salih: investigation and methodology. Xinyu Wang and Peter R. Corridon: resources, methodology and writing-review & editing. Khalil B. Ramadi: writing-review & editing. Haider Butt: supervision, fund acquisition, and project administration.

Conflicts of interest

The authors declare no competing interests.

Acknowledgements

The authors acknowledge the Khalifa University of Science and Technology (KUST) and the KU-KAIST Joint Research Center for research funding in support of this research (Project code: 8474000220-KKJRC-2019-Health1). P. C. acknowledges Dr. Fayez Al Masalmeh and Dr. Abdalla Elsayed Elshikh for support and approval to obtain tissue samples from the Abu Dhabi Automated Slaughterhouse, Abu Dhabi City Municipality.

References

1 T. A. Kurniawan, G. Y. Chan, W.-H. Lo and S. Babel, Physico–chemical treatment techniques for wastewater laden with heavy metals, *Chem. Eng. J.*, 2006, **118**(1–2), 83–98.
2 M. Galbe and G. Zacchi, Pretreatment: the key to efficient utilization of lignocellulosic materials, *Biomass Bioenergy*, 2012, **46**, 70–78.
3 P. Paroutis, N. Touret and S. Grinstein, The pH of the secretory pathway: measurement, determinants, and regulation, *Physiology*, 2004, **19**(4), 207–215.
4 X. Zhang, Y. Lin and R. J. Gillies, Tumor pH and its measurement, *J. Nucl. Med.*, 2010, **51**(8), 1167–1170.
5 H. Izumi, T. Torigoe, H. Ishiguchi, H. Uramoto, Y. Yoshida, M. Tanabe, T. Ise, T. Murakami, T. Yoshida, M. Nomoto and K. Kohno, Cellular pH regulators: potentially promising molecular targets for cancer chemotherapy, *Cancer Treat. Rev.*, 2003, **29**, 541–549.
6 T. Nishi and M. Forgac, The vacuolar (H+)-ATPases—nature's most versatile proton pumps, *Nat. Rev. Mol. Cell Biol.*, 2002, **3**(2), 94–103.
7 H. Galster, *pH measurement*, VCH (Verlagsgesellschaft), New York, 1991.
8 A. A. Belyustin, The centenary of glass electrode: from Max Cremer to FGK Baucke, *J. Solid State Electrochem.*, 2011, **15**(1), 47–65.
9 M. R. Hartings, N. J. Castro, K. Gill and Z. Ahmed, A photonic pH sensor based on photothermal spectroscopy, *Sens. Actuators, B*, 2019, **301**, 127076.
10 R. Wang, C. Yu, F. Yu and L. Chen, Molecular fluorescent probes for monitoring pH changes in living cells, *TrAC, Trends Anal. Chem.*, 2010, **29**(9), 1004–1013.
11 S. Udomsom, A. Budwong, C. Wongsa, P. Sangngam, P. Baipaywad, C. Manaspon, S. Auephanwiriyakul, N. Theera-Umpon and P. Paengnakorn, Automatic Programmable Bioreactor with pH Monitoring System for Tissue Engineering Application, *Bioengineering*, 2022, **9**(5), 187.
12 J. F. Welter and H. Baskaran, Monitoring and real-time control of tissue engineering systems, in *Principles of Tissue Engineering*, 2020, Elsevier, pp. 1459–1467.
13 S. K. Parks, J. Chiche and J. Pouyssegur, pH control mechanisms of tumor survival and growth, *J. Cell. Physiol.*, 2011, **226**(2), 299–308.
14 J. Zhang, B. A. Doll, E. J. Beckman and J. O. Hollinger, A biodegradable polyurethane-ascorbic acid scaffold for bone tissue engineering, *J. Biomed. Mater. Res., Part A*, 2003, **67**(2), 389–400.
15 W. Vonau and U. Guth, pH monitoring: a review, *J. Solid State Electrochem.*, 2006, **10**, 746–752.

16 M. Anderson, A. Moshnikova, D. M. Engelman, Y. K. Reshetnyak and O. A. Andreev, Probe for the measurement of cell surface pH in vivo and ex vivo, *Proc. Natl. Acad. Sci. U. S. A.*, 2016, **113**(29), 8177–8181.

17 A. A. Pezzulo, X. X. Tang, M. J. Hoegger, M. H. Abou Alaiwa, S. Ramachandran, T. O. Moninger, P. H. Karp, C. L. Wohlford-Lenane, H. P. Haagsman and M. van Eijk, Reduced airway surface pH impairs bacterial killing in the porcine cystic fibrosis lung, *Nature*, 2012, **487**(7405), 109–113.

18 W. Paschen, B. Djuricic, G. Mies, R. Schmidt-Kastner and F. Linn, Lactate and pH in the brain: association and dissociation in different pathophysiological states, *J. Neurochem.*, 1987, **48**(1), 154–159.

19 R. R. Kedika, R. F. Souza and S. J. Spechler, Potential anti-inflammatory effects of proton pump inhibitors: a review and discussion of the clinical implications, *Dig. Dis. Sci.*, 2009, **54**(11), 2312–2317.

20 J. Lin, Recent development and applications of optical and fiber-optic pH sensors, *TrAC, Trends Anal. Chem.*, 2000, **19**(9), 541–552.

21 D. Wencel, T. Abel and C. McDonagh, Optical chemical pH sensors, *Anal. Chem.*, 2014, **86**(1), 15–29.

22 V. Moradi, M. Akbari and P. Wild, A fluorescence-based pH sensor with microfluidic mixing and fiber optic detection for wide range pH measurements, *Sens. Actuators, A*, 2019, **297**, 111507.

23 T. H. Nguyen, T. Venugopala, S. Chen, T. Sun, K. T. Grattan, S. E. Taylor, P. M. Basheer and A. E. Long, Fluorescence based fibre optic pH sensor for the pH 10–13 range suitable for corrosion monitoring in concrete structures, *Sens. Actuators, B*, 2014, **191**, 498–507.

24 J. Janata, Do optical sensors really measure pH?, *Anal. Chem.*, 1987, **59**(9), 1351–1356.

25 T. H. Nguyen, T. Venugopalan, T. Sun and K. T. Grattan, Intrinsic fiber optic pH sensor for measurement of pH values in the range of 0.5–6, *IEEE Sens. J.*, 2015, **16**(4), 881–887.

26 T. Liu, W. Wang, H. Ding and D. Yi, Smartphone-based hand-held optical fiber fluorescence sensor for on-site pH detection, *IEEE Sens. J.*, 2019, **19**(20), 9441–9446.

27 M. Rosenberg, B. W. Laursen, C. G. Frankær and T. J. Sørensen, A fluorescence intensity ratiometric fiber optics–based chemical sensor for monitoring pH, *Adv. Mater. Technol.*, 2018, **3**(12), 1800205.

28 R. Kumar, H. Nguyen, B. Rente, C. Tan, T. Sun and K. T. Grattan, A portable 'plug-and-play'fibre optic sensor for in-situ measurements of pH values for microfluidic applications, *Micromachines*, 2022, **13**(8), 1224.

29 B. Zhou, K. Fan, T. Li, G. Luan and L. Kong, A biocompatible hydrogel-coated fiber-optic probe for monitoring pH dynamics in mammalian brains in vivo, *Sens. Actuators, B*, 2023, 133334.

30 M. Gao and B. Z. Tang, Fluorescent sensors based on aggregation-induced emission: recent advances and perspectives, *ACS Sens.*, 2017, **2**(10), 1382–1399.

31 J. Han and K. Burgess, Fluorescent indicators for intracellular pH, *Chem. Rev.*, 2010, **110**(5), 2709–2728.

32 L. Liu, P. Guo, L. Chai, Q. Shi, B. Xu, J. Yuan, X. Wang, X. Shi and W. Zhang, Fluorescent and colorimetric detection of pH by a rhodamine-based probe, *Sens. Actuators, B*, 2014, **194**, 498–502.

33 N. Raoufi, F. Surre, M. Rajarajan, T. Sun and K. T. Grattan, Fiber optic pH sensor using optimized layer-by-layer coating approach, *IEEE Sens. J.*, 2013, **14**(1), 47–54.

34 F. Surre, W. Lyons, T. Sun, K. Grattan, S. O'Keeffe, E. Lewis, C. Elosua, M. Hernaez and C. Barian, U-bend fibre optic pH sensors using layer-by-layer electrostatic self-assembly technique, *J. Phys.: Conf. Ser.*, 2009, **178**, 012046.

35 N. Othman, W. F. Hanim, U. M. Noor and S. Hana, Optical pH sensor based on polyaniline sol-gel film immobilized with bromothymol blue and phenol red, *AIP Conf. Proc.*, 2016, **1774**(1), 050014.

36 H. Khanjanzadeh, B.-D. Park and H. Pirayesh, Intelligent pH-and ammonia-sensitive indicator films using neutral red immobilized onto cellulose nanofibrils, *Carbohydr. Polym.*, 2022, **296**, 119910.

37 J. Goicoechea, C. Zamarreño, I. Matias and F. Arregui, Optical fiber pH sensors based on layer-by-layer electrostatic self-assembled Neutral Red, *Sens. Actuators, B*, 2008, **132**(1), 305–311.

38 F. J. Arregui, I. Latasa, I. R. Matias and R. O. Claus, An optical fiber pH sensor based on the electrostatic self-assembly method, in *SENSORS, 2003 IEEE*, IEEE, 2003.

39 P. W. Kirk, Neutral red as a lipid fluorochrome, *Stain Technol.*, 1970, **45**(1), 1–4.

40 V. Bhardwaj, A. K. Pathak and V. K. Singh, No-core fiber-based highly sensitive optical fiber pH sensor, *J. Biomed. Opt.*, 2017, **22**(5), 057001.

41 A. Seki, H. Katakura, T. Kai, M. Iga and K. Watanabe, A hetero-core structured fiber optic pH sensor, *Anal. Chim. Acta*, 2007, **582**(1), 154–157.

42 Y. Yang, X. Yang, Y.-L. Liu, Z.-M. Liu, H.-F. Yang, G.-L. Shen and R.-Q. Yu, Optical sensor for lithocholic acid based on multilayered assemblies from polyelectrolyte and cyclodextrin, *J. Photochem. Photobiol., A*, 2005, **171**(2), 137–144.

43 A. B. Ganesh and T. Radhakrishnan, Fiber-optic pH sensor, *Fiber Integr. Opt.*, 2006, **25**(6), 403–409.

44 S. A. Grant, K. Bettencourt, P. Krulevitch, J. Hamilton and R. Glass, In vitro and in vivo measurements of fiber optic and electrochemical sensors to monitor brain tissue pH, *Sens. Actuators, B*, 2001, **72**(2), 174–179.

45 E. C. Mackle, J. M. Coote, E. Carr, C. D. Little, G. van Soest and A. E. Desjardins, Fibre optic intravascular measurements of blood flow: A review, *Sens. Actuators, A*, 2021, **332**, 113162.

46 R. Bockholt, S. Paschke, L. Heubner, B. Ibarlucea, A. Laupp, Ž. Janićijević, S. Klinghammer, S. Balakin, M. F. Maitz and C. Werner, Real-time monitoring of blood parameters in the intensive care unit: State-of-the-art and perspectives, *J. Clin. Med.*, 2022, **11**(9), 2408.

47 M. Menzel, J. Soukup, D. Henze, K. Engelbrecht, M. Senderreck, A. Scharf, A. Rieger and S. Grond, Experiences with continuous intra-arterial blood gas monitoring: precision and drift of a pure optode-system, *Intensive Care Med.*, 2003, **29**, 2180–2186.